# Acute selective ablation of rat insulin promoter-expressing ($RIP_{HER}$) neurons defines their orexigenic nature

Eva Rother[a,b], Bengt F. Belgardt[a,c], Eva Tsaousidou[a,c], Brigitte Hampel[a,c], Ari Waisman[d], Martin G. Myers, Jr.[e], and Jens C. Brüning[a,b,c,1]

[a]Institute for Genetics, Department of Mouse Genetics and Metabolism, Center for Molecular Medicine (CMMC), and Cologne Excellence Cluster on Cellular Stress Responses in Aging-Associated Diseases (CECAD), University of Cologne, 50674 Cologne, Germany; [b]Center for Endocrinology, Diabetes and Preventive Medicine, University Hospital Cologne, 50924 Cologne, Germany; [c]Max Planck Institute for Neurological Research, 50931 Cologne, Germany; [d]Institute for Molecular Medicine, University Medical Center of the Johannes Gutenberg University of Mainz, 55131 Mainz, Germany; and [e]Division of Metabolism, Endocrinology, and Diabetes, Department of Internal Medicine, and Department of Molecular and Integrative Physiology, University of Michigan, Ann Arbor, MI 48105

Edited by Tamas L. Horvath, Yale University School of Medicine, New Haven, CT, and accepted by the Editorial Board September 7, 2012 (received for review April 12, 2012)

**Rat insulin promoter (RIP)-expressing neurons in the hypothalamus control body weight and energy homeostasis. However, genetic approaches to study the role of these neurons have been limited by the fact that RIP expression is predominantly found in pancreatic β-cells, which impedes selective targeting of neurons. To define the function of hypothalamic RIP-expressing neurons, we set out to acutely and selectively eliminate them via diphtheria toxin-mediated ablation. Therefore, the diphtheria toxin receptor transgene was specifically expressed upon RIP-specific Cre recombination using a RIP-Cre line first described by Herrera ($RIP_{HER}$-Cre) [Herrera PL (2000) *Development* 127:2317–2322]. Using proopiomelanocortin–expressing cells located in the arcuate nucleus of the hypothalamus and in the pituitary gland as a model, we established a unique protocol of intracerebroventricular application of diphtheria toxin to efficiently ablate hypothalamic cells with no concomitant effect on pituitary proopiomelanocortin–expressing corticotrophs in the mouse. Using this approach to ablate $RIP_{HER}$ neurons in the brain, but not in the pancreas, resulted in decreased food intake and loss of body weight and fat mass. In addition, ablation of $RIP_{HER}$ neurons caused increased c-Fos immunoreactivity of neurons in the paraventricular nucleus (PVN) of the hypothalamus. Moreover, transsynaptic tracing of $RIP_{HER}$ neurons revealed labeling of neurons located in the PVN and dorsomedial hypothalamic nucleus. Thus, our experiments indicate that $RIP_{HER}$ neurons inhibit anorexigenic neurons in the PVN, revealing a basic orexigenic nature of these cells.**

neuroscience | obesity

The mammalian brain regulates energy balance in response to peripheral signals from the pancreas, adipose tissue, and the intestinal tract (1–3). More than 60 y ago, cerebral lesion and stimulation studies identified specific hypothalamic nuclear regions involved in this action (4, 5). More recently, the rapidly evolving technology to generate and analyze transgenic mice has provided new avenues of investigating the specific role of a defined cell population by targeted cell ablation. Approaches to achieve targeted cell ablation include the disruption of genes required for the development or survival of the particular cell lineage (6) or lineage-restricted expression of a cytotoxic protein, such as the diphtheria toxin A subunit (DT-A) (7, 8). More recent developments have even allowed for the timely controlled ablation of cells by cell type-restricted transgenic expression of the diphtheria toxin receptor (DTR) and subsequent administration of diphtheria toxin (DT) (9–12).

Previously, we have successfully used this approach to investigate the role of the melanocortin system in energy homeostasis using mice expressing the DTR selectively in proopiomelanocortin (POMC)-expressing neurons ($POMC^{DTR}$ mice) (13). POMC is generated in a subset of hypothalamic and hindbrain neurons as well as in the melanotrophs and corticotrophs of the pituitary gland, and processed posttranslationally to yield ACTH and α-, β- and γ-melanocyte–stimulating hormones (MSH) (14–19). Our experiments demonstrated that the acute systemic destruction of POMC-expressing cells in adult mice results in hyperphagia and obesity accompanied by severe hypocortisolism. Thus, DT-induced ablation of defined neurons by transgenic expression of the DTR provides a powerful tool to investigate the role of specific neuronal subpopulations in a biological context.

However, this approach is often limited by the fact that although certain promoters exhibit a highly restricted expression pattern to direct DTR expression within the CNS, they are also active in peripheral tissues. Thus, systemic application of DT leads to cell ablation in any tissue expressing the receptor; for $POMC^{DTR}$ mice, this results in simultaneous loss of hypothalamic and pituitary POMC cells and thus in counteracting effects on energy homeostasis via altered levels of ACTH-dependent glucocorticoid hormones (i.e., corticosterone), which regulate metabolism, fat distribution, and the development of obesity independently of α-MSH (18, 20). Therefore, systemic POMC cell ablation cannot be used to study the net effect of hypothalamic POMC cells on energy homeostasis.

Besides POMC neurons, other hypothalamic neuronal populations are essential for adequate control of energy homeostasis. Analysis of mice harboring a rat insulin II promoter-Cre transgene revealed Cre-mediated expression of a reporter gene in a poorly described neuronal hypothalamic population (21). It has been suggested that these so-called rat insulin promoter (RIP) neurons play a role in melanocortinergic control of body weight or are even POMC neurons, but other studies have found no overlap of RIP-Cre and POMC expression (22). RIP-expressing neurons seem to be primary targets of insulin and leptin because mice, upon RIP cell-specific deletion of either insulin receptor substrate (IRS) 2 or signal transducer and activator of transcription (STAT) 3, develop impaired glucose tolerance and altered food intake (22, 23). Moreover, these findings that are not readily explained by IRS 2 and STAT 3 action in pancreatic β-cells. Interestingly, insulin and MTII (an α-MSH mimetic), but not leptin, depolarized and increased spiking of RIP neurons (22). When the anorexigenic effect of insulin and α-MSH is taken into consideration, the activation of RIP neurons would be expected to decrease food intake and

Author contributions: J.C.B. designed research; E.R., B.F.B., E.T., and B.H. performed research; A.W. and M.G.M. contributed new reagents/analytic tools; E.R., B.F.B., and E.T. analyzed data; and E.R., B.F.B., and J.C.B. wrote the paper.

The authors declare no conflict of interest.

This article is a PNAS Direct Submission. T.L.H. is a guest editor invited by the Editorial Board.

[1]To whom correspondence should be addressed. E-mail: bruening@nf.mpg.de.

This article contains supporting information online at www.pnas.org/lookup/suppl/doi:10.1073/pnas.1206147109/-/DCSupplemental.

define the anorexigenic nature of this cell population. Nonetheless, data from all mouse models concerning RIP-expressing neurons to date suffer from possible side effects of Cre-mediated recombination in β-cells of RIP-Cre mice and/or from compensatory developmental mechanisms. Complicating matters, different lines of RIP-Cre transgenic mice exhibit different recombination patterns in the hypothalamus, from broad-based recombination in the transgenic mouse strain, initially described by Magnuson and colleagues ($RIP_{MAG}$-Cre) (21), to that generated by the Herrera group ($RIP_{HER}$-Cre), which results in recombination in a distinct population of cells mainly located in the arcuate nucleus (ARC) of the hypothalamus (24, 25). To better define the function of the latter group of hypothalamic RIP neurons, which exhibit a more restricted pattern in the ARC, we set out to acutely ablate $RIP_{HER}$ neurons without concurrent ablation of pancreatic β-cells.

To identify the correct dosage for central, but not systemic, ablation of $RIP_{HER}$ (or any other population of hypothalamic) cells, we reasoned that intracerebroventricular (icv) injection of DT in mice with POMC cell-restricted expression of the DTR ($POMC^{DTR}$ mice) would allow the most sensitive readout because (*i*) the hypothalamus and pituitary are located in close proximity and (*ii*) both hypothalamic and pituitary POMC cell number and mRNA can be readily assessed using GFP reporter mice and gene expression analysis, respectively. Thus, studies of hypothalamus-restricted action of icv-administered DT in mice with $RIP_{HER}$ cell-restricted expression of the DTR should ultimately reveal the role of $RIP_{HER}$ neurons in the regulation of energy homeostasis.

## Results

**CNS-Specific Ablation of Hypothalamic POMC Cells.** To selectively ablate POMC neurons located in the ARC while sparing peripheral POMC-expressing cells, we applied 0.6 ng of DT directly to the cerebral ventricular system of $POMC^{DTR/LacZ}$ and control ($POMC^{LacZ}$) mice. Efficacy of ablation was assessed by quantification of β-galactosidase–expressing POMC neurons in tissue sections of hypothalami of $POMC^{DTR/LacZ}$ and control animals 15 d after DT treatment. After central ablation, the average POMC cell count per hypothalamic tissue section was reduced by 90% in $POMC^{DTR}$ mice injected with 0.6 ng DT compared with controls (Fig. 1 *A* and *B*). Systemic ablation even reduced the number of stainable POMC neurons to less than 1% (Fig. 1*A* and *B*). Hypothalamic POMC mRNA expression in $POMC^{DTR}$ mice 15 d after DT treatment was reduced by 81% and 83% after 0.6 ng DT (icv) and 40 ng/g body weight DT (ip), respectively (Fig. 1*C*). Selectivity of hypothalamic ablation was analyzed by quantification of pituitary POMC mRNA levels and serum corticosterone levels. In $POMC^{DTR}$ animals receiving systemic DT treatment, we observed a dramatic 72% reduction of pituitary POMC mRNA levels compared with DT-treated control animals (Fig. 1*D*). In addition, we found a massive decrease of serum corticosterone levels in $POMC^{DTR}$ mice 15 d after ip DT treatment, whereas corticosterone levels in control animals remained unchanged throughout the experiment (Fig. 1*E*). In contrast, $POMC^{DTR}$ mice receiving 0.6 ng icv DT treatment showed no change in either pituitary POMC mRNA or serum corticosterone levels (Fig. 1 *D* and *E*). Taken together, icv application of 0.6 ng DT did not affect pituitary POMC cell function, whereas systemic DT treatment drastically compromised pituitary POMC cell number and function as assessed by pituitary POMC mRNA and serum corticosterone levels.

Icv application of DT resulted in increased body weight in $POMC^{DTR}$ animals, which gained ~7.0% of their starting weight within 15 d after DT treatment, whereas control animals remained unaffected (Fig. 1*F*). $POMC^{DTR}$ animals that underwent systemic ablation showed a milder increase in body weight of only 3.1% (Fig. 1*F*). Differences in body weight between both groups of $POMC^{DTR}$ and controls were significant ($P < 0.0001$; Fig. 1*F*). Strikingly, $POMC^{DTR}$ animals receiving 0.6 ng icv were also significantly heavier than $POMC^{DTR}$ animals undergoing systemic ablation ($P < 0.001$), and increased food intake was most prominent in $POMC^{DTR}$ mice treated with 0.6 ng DT icv ($P < 0.0001$; Fig. 1*G*).

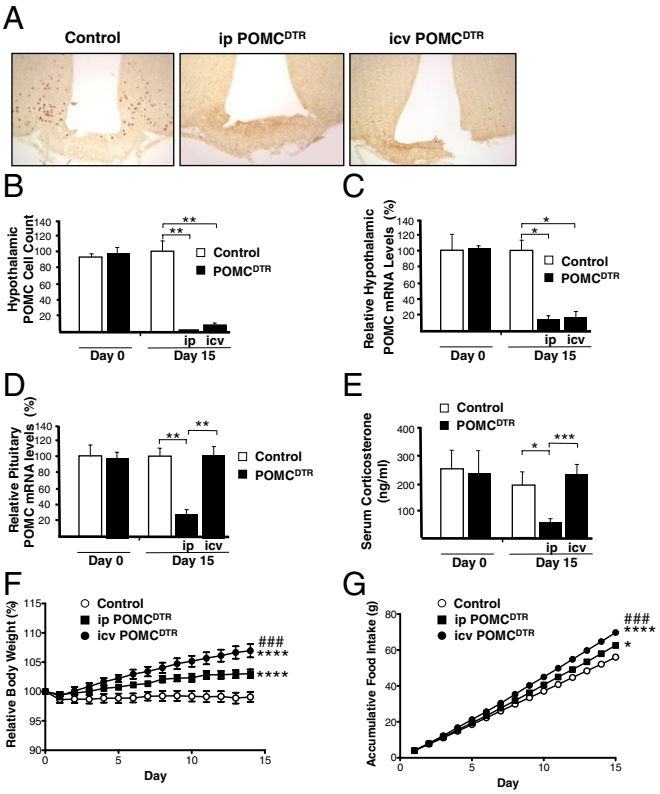


**Fig. 1.** Systemic and CNS-specific ablation of hypothalamic POMC cells. (*A*) β-galactosidase staining of control and $POMC^{DTR}$ mice 15 d after either systemic treatment with 40 ng/g body weight DT ip or central icv treatment with 0.6 ng DT. (*B*) Hypothalamic POMC cell count (both hemispheres), (*C*) relative hypothalamic POMC mRNA levels (%), (*D*) relative pituitary POMC mRNA levels (%), and (*E*) serum corticosterone levels (ng/mL) before and 15 d after systemic DT treatment in control and $POMC^{DTR}$ animals that received either systemic (ip) or central (icv) DT treatment. (*F*) Relative body weight and (*G*) accumulative food intake over the 15-d period after systemic and central DT treatment in $POMC^{DTR}$ animals receiving 0.6 ng DT icv (●), $POMC^{DTR}$ animals undergoing systemic ablation (■), and control animals (○). Displayed values are means ± SEM of 8–12 animals per group, $*P \leq 0.05$, $***P \leq 0.001$, $****P \leq 0.0001$ of the respective experimental group compared with control animals. $^{###}P \leq 0.001$ $POMC^{DTR}$ icv ablation vs. $POMC^{DTR}$ systemic ablation.

**Glucose Tolerance in Systemic and Central Ablation of $RIP_{HER}$ Cells.** To study the role of hypothalamic $RIP_{HER}$ neurons, we generated mice heterozygous both for Cre under the transcriptional control of the rat insulin II promoter (25) as well as the DTR allele. To establish a reporter mouse line, we generated mice with an additional Cre-activatable GFP allele (26). As systemic application of DT would likely lead to ablation of pancreatic insulin-producing β-cells, we measured blood glucose concentrations during the experiments in all three groups. Systemic ablation of $RIP_{HER}$ cells led to significantly increased blood glucose concentrations 2 d after treatment, with concentrations of 600 mg/dL being reached after 6 d (Fig. 2*A*). Interestingly, treatment with 0.6 ng DT icv did not lead to any changes in blood glucose levels compared with controls (Fig. 2*A*). We next determined serum insulin levels in all three groups 8 d after DT treatment. Systemic ablation of $RIP_{HER}$ cells was observed to lead to a significant decrease in circulating insulin concentration, whereas no difference between control and mice with central ablation was detected (Fig. 2*B*). To next investigate how systemic and central

NEUROSCIENCE

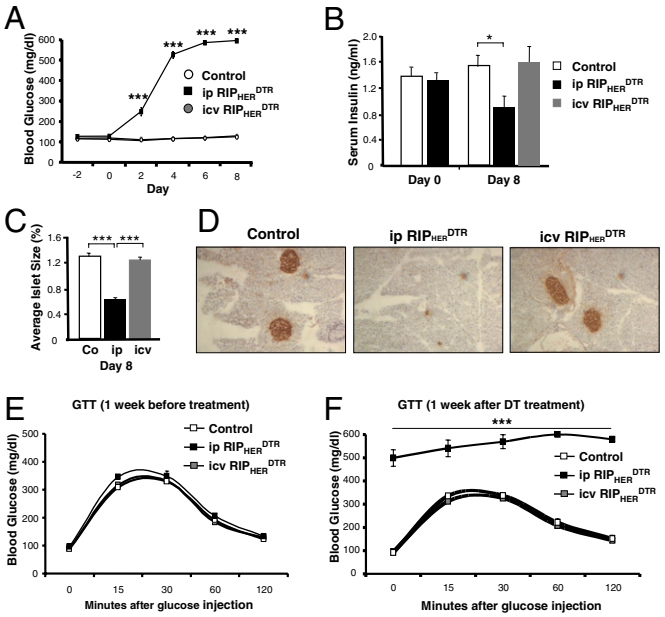


**Fig. 2.** Glucose tolerance in systemic and central ablation of $RIP_{HER}$ cells. (*A*) Random-fed blood glucose levels in control, DT ip-injected $RIP_{HER}^{DTR}$, and DT icv-injected $RIP_{HER}^{DTR}$ mice 2 d before treatment until 8 d after treatment. (*B*) Serum insulin levels in control and $RIP_{HER}^{DTR}$ animals that received either systemic (ip) or central (icv) DT treatment immediately before DT treatment and 8 d after DT treatment. (*C*) Average islet size in control and $RIP_{HER}^{DTR}$ animals that received either systemic (ip) or central (icv) DT treatment 8 d after treatment. Representative images of islets are shown in *D*. (*E*) Glucose tolerance test in control, ip-injected $RIP_{HER}^{DTR}$ and icv-injected $RIP_{HER}^{DTR}$ mice 1 wk before treatment. (*F*) Glucose tolerance test (GTT) in control, ip-injected $RIP_{HER}^{DTR}$, and icv-injected $RIP_{HER}^{DTR}$ mice 1 wk after treatment. Displayed values are means ± SEM of 5–8 animals per group. ***$P \leq 0.001$ between the indicated groups.

ablation of $RIP_{HER}$ cells affected pancreatic insulin-producing β-cells, we assessed pancreatic β-cell mass in all three treatment groups. Systemic ablation of $RIP_{HER}$ cells significantly decreased β-cell mass, whereas central ablation by injection of 0.6 ng DT had no effect on β-cell mass compared with controls (Fig. 2 *C* and *D*). We then performed glucose tolerance tests in all three groups and found no difference in glucose tolerance test (GTT) performance before DT treatment (Fig. 2*E*). Systemic ablation of $RIP_{HER}$ cells induced absolute glucose intolerance as evidenced by mean fasting glucose concentrations of 500 mg/dL that even exceeded the detection limit of 600 mg/dL after glucose injection (Fig. 2*F*). In stark contrast, central ablation of $RIP_{HER}$ cells did not affect glucose tolerance compared with controls (Fig. 2*F*). Taken together, systemic but not central ablation of $RIP_{HER}$ cells induces loss of β-cells and subsequent glucose intolerance.

**Central Ablation of $RIP_{HER}$ Neurons Causes Hypophagia and Weight Loss.** We next quantitatively assessed the ablation of hypothalamic $RIP_{HER}$ neurons using GFP reporter mice. In control reporter mice ($RIP_{HER}^{GFP}$), GFP-positive cells were detected throughout the ARC with an average number of ∼30 cells per 25-μm section (Fig. 3 *A* and *B*). Both systemic and central ablation of $RIP_{HER}$ neurons induced a significant and equal loss of hypothalamic $RIP_{HER}$ neurons after 8 d, as determined by immunohistological analysis of GFP-positive cells (Fig. 3 *A* and *B*). We next assessed the effect of systemic and central ablation of $RIP_{HER}$ cells on body weight and food intake. Systemic ablation of $RIP_{HER}$ cells induced 10% weight loss after 8 d (Fig. 3*C*). This observation was concurrent with unchanged food intake compared with controls and is thus likely an effect of urine glucose loss due to uncontrolled diabetes (Fig. 3*D*). Surprisingly, central ablation of $RIP_{HER}$ cells also led to a 10% decrease in body weight along with a significant decrease in food intake (Fig. 3 *C* and *D*). To ensure that the decrease in body weight was not due to loss of lean mass, we used in vivo NMR analysis and found a significant decrease in body fat percentage in centrally ablated mice compared with controls (Fig. 3*E*). Consistently, leptin levels were significantly decreased in these mice compared with controls (Fig. 3*F*). Taken together, central $RIP_{HER}$ cell deletion leads to hypophagia and subsequently decreased adiposity.

Real-time PCR analysis of gene expression in the ventromedial hypothalamus (VMH) revealed no differential expression of orexigenic neuropeptide Y (NPY), anorexigenic BDNF, or steroidogenic factor (SF)1, which are key neuropeptides involved in energy homeostasis (NPY and BDNF) or implicated in VMH development and maintenance (SF1). In microdissections of the ARC, expression of anorexigenic POMC was slightly decreased,

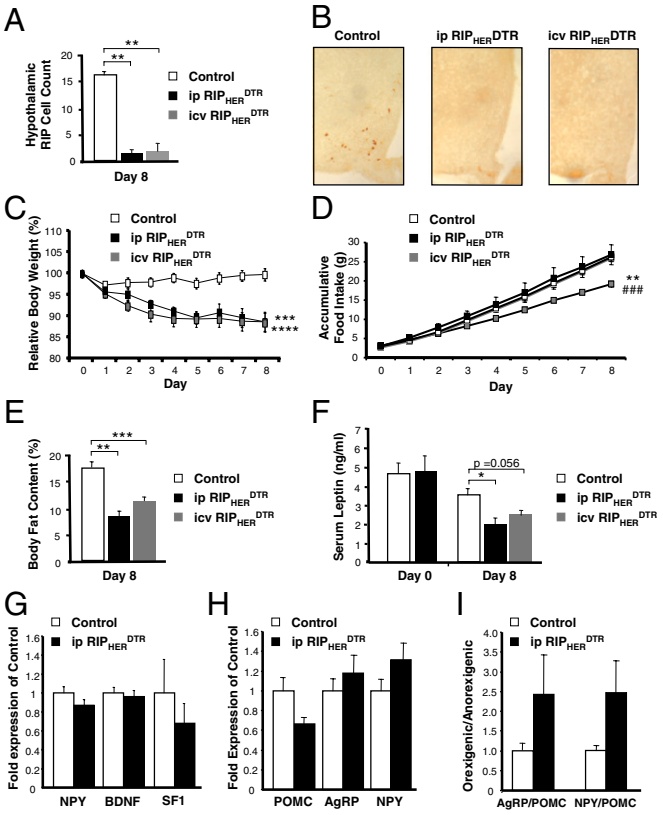


**Fig. 3.** Central ablation of $RIP_{HER}$ neurons causes hypophagia and weight loss. (*A*) Hypothalamic $RIP_{HER}$ cell counts (per hemisphere) in $RIP_{HER}^{DTR/GFP}$ reporter mice treated with saline (control), 40 ng/g body weight ip (systemic ablation), or 0.6 ng icv (central ablation) 8 d after treatment. Representative images are shown in *B*. (*C*) Development of relative body weight mass until 8 d after ip or icv DT treatment in $RIP_{HER}^{DTR}$ mice. Individual body weight immediately before DT treatment was set as 100%, and body weight was individually calculated as percentage of starting body weight. (*D*) Accumulative food intake in control and in $RIP_{HER}^{DTR}$ mice over 8 d after ip or icv DT treatment. (*E*) Body fat content of control mice and $RIP_{HER}^{DTR}$ mice 8 d after ip or icv DT treatment. (*F*) Serum leptin levels of control mice and $RIP_{HER}^{DTR}$ mice after ip or icv DT treatment. (*G*) mRNA expression of NPY, BDNF, and steroidogenic factor 1 (SF1) in microdissected ventromedial hypothalamic nuclei of control and $RIP_{HER}^{DTR}$ mice 8 d after icv DT treatment. (*H*) mRNA expression of POMC, AgRP, and NPY in microdissected hypothalamic ARC of control and $RIP_{HER}^{DTR}$ mice 8 d after icv DT treatment. (*I*) Ratio of orexigenic (AgRP and NPY) vs. anorexigenic (POMC) neuropeptide mRNA expression in microdissected hypothalamic ARC of control and $RIP_{HER}^{DTR}$ mice 8 d after icv DT treatment. Displayed values are means ± SEM of 8–12 animals per group, *$P \leq 0.05$, **$P \leq 0.01$, ***$P \leq 0.001$, and ****$P \leq 0.0001$ for the respective experimental group vs. control animals; $^{\#\#\#}P \leq 0{,}001$ for $RIP_{HER}^{DTR}$ icv ablation vs. $RIP_{HER}^{DTR}$ systemic ablation.

whereas expression of orexigenic neuropeptides [agouti-related peptide (AgRP) and NPY] was mildly increased upon central $RIP_{HER}$ cell ablation (Fig. 3*H*). The relation of orexigenic to anorexigenic neuropeptide expression, however, indicates a clear tendency toward an orexigenic tone of neuropeptide expression in the ARC following $RIP_{HER}$ cell ablation, which is consistent with lowered circulating plasma leptin concentrations (Fig. 3*I*).

**Ablation of $RIP_{HER}$ Neurons Activates Paraventricular Nucleus Neurons.** To further identify possible downstream target nuclei involved in mediating the orexigenic drive of $RIP_{HER}$ neurons, we assessed neuronal activation using the surrogate marker c-Fos in multiple hypothalamic and extrahypothalamic nuclei 2 d after icv DT application. This analysis revealed a significantly increased number of c-Fos–expressing neurons in the paraventricular nucleus (PVN) following $RIP_{HER}$ cell ablation, indicating increased neuronal activity of PVN neurons (Fig. 4*A*). In contrast, c-Fos expression was unaltered in the ARC, lateral hypothalamus (LH), or VMH. Furthermore, changes in c-Fos expression were not detectable in extrahypothalamic brain regions. Note that in the ARC, high numbers of c-Fos–positive neurons were observed in $RIP_{HER}^{DTR}$ as well as control animals.

To investigate whether PVN neurons receive synaptic input from $RIP_{HER}$ cells, we next aimed to visualize synaptic connectivity of $RIP_{HER}$ cells. To this end, $RIP_{HER}$-Cre mice were crossed with mice that express wheat germ agglutinin (WGA), a lectin that passes transsynaptically and accumulates in target neurons, downstream of the CMV promoter-driven floxed β-geo cassette and upstream of an internal ribosome entry site–alkaline phosphatase (AP) sequence (Fig. S1*A*) (27, 28). Subsequent staining of brain sections from adult double-heterozygous ($RIP_{HER}^{WGA}$) and control mice revealed unspecific immunoreactivity in an area adjacent to the ARC and VMH in $RIP_{HER}^{WGA}$ mice as well as control mice, which only carried the WGA transgene in the absence of the $RIP_{HER}$-Cre transgene (Fig. S1*B*). However, further careful analysis for WGA immunoreactivity within other nuclear regions of the hypothalamus revealed specific WGA immunoreactivity in a proportion of PVN neurons and dorsomedial hypothalamic (DMH) neurons only of $RIP_{HER}^{WGA}$ mice but not in control animals (Fig. 4*B* and Fig. S1*C*). Other examined nuclei (ARC and LH) failed to exhibit WGA immunoreactivity in both $RIP_{HER}^{WGA}$ and control mice (Fig. S1*C*). Thus, $RIP_{HER}$ neuronal targeting of second-order neurons in the PVN and DMH in conjunction with the increased c-Fos expression upon ablation of $RIP_{HER}$ neurons indicates that $RIP_{HER}$ neurons inhibit neuronal activation in the PVN.

## Discussion

Ever since the first lesion studies identified certain nuclear regions of the hypothalamus as major sites of energy homeostasis regulation, tremendous effort has been put into promoting our fundamental understanding of the central structures and neuronal circuits involved in this regulatory process. In the present study, we introduce a unique approach to effectively, acutely, and selectively ablate hypothalamic cells. Detailed characterization of genetically engineered mice expressing a DTR selectively in $POMC^{DTR}$ that received central DT treatment proved brain-restricted DT-induced ablation. Icv application of only 0.6 ng DT in $POMC^{DTR}$ mice led to effective and selective destruction of hypothalamic POMC neurons while equally susceptible pituitary POMC cells were left unaffected. In addition, mice centrally receiving DT presented the strongest increase in food intake and body weight throughout the 15-d observation period. This effect can be explained by unaffected corticosterone production and, hence, permissive action of corticosterone on the modulation of appetite, metabolism, and energy partitioning in addition to hypothalamic deficiency of POMC. These results clearly show an effective and selective ablation of a defined central cell population without affecting cells expressing DTR in the periphery.

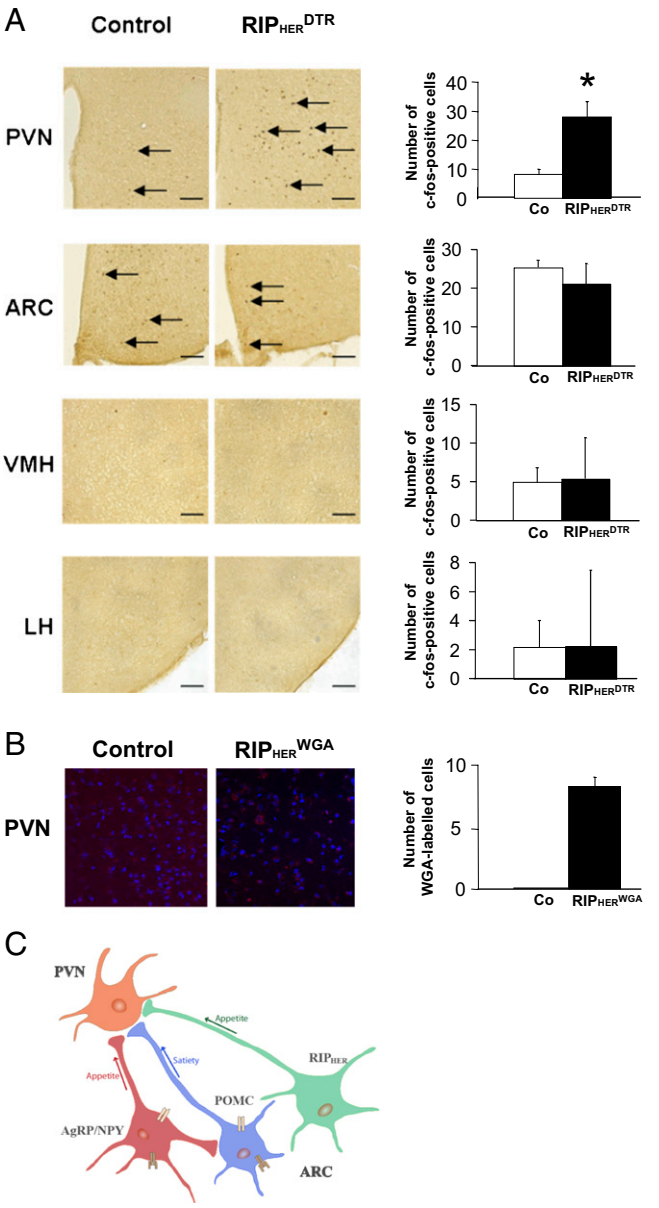


**Fig. 4.** $RIP_{HER}$ neurons target the PVN. (*A*) Detection of neuronal activity by c-Fos immunohistochemistry. Control and $RIP_{HER}^{DTR}$ mice were icv injected with DT and killed 48 h later. Immunohistochemistry was performed for the surrogate marker for neuronal activity, c-Fos. Significantly increased numbers of c-Fos–positive neurons per hemisphere in the PVN, but not the ARC, the VMH, or the LH of $RIP_{HER}^{DTR}$ mice were observed. Arrows depict c-Fos–positive neurons in $RIP_{HER}^{DTR}$ and control mice. (Scale bar: 100 μm.) (*B*) Transsynaptic tracing study by staining for WGA in mice with conditional expression of WGA in $RIP_{HER}$ neurons ($RIP_{HER}^{WGA}$ mice). Representative staining of WGA-positive neurons (red) in the PVN of $RIP_{HER}^{WGA}$ and control mice. Average cell count of WGA-labeled cells in the PVN (both hemispheres). (*C*) Hypothesized role of $RIP_{HER}$-expressing neurons. $RIP_{HER}$ neurons might exert part of their orexigenic function via direct inhibition on anorexigenic second order neurons of the PVN.

Recent findings have suggested that arcuate RIP-expressing neurons are targets for insulin and melanocortins (22). Systemic manipulation of RIP-expressing cells results in a phenotype that is dominated by the effect on β-cell function, whereas the central effects are masked. Thus, the net effect of RIP-expressing neurons on energy homeostasis could so far not be defined. We used the systemic vs. central ablation approach to identify the roles of

NEUROSCIENCE

central RIP cells on energy homeostasis without perturbations stemming from β-cell loss. Strikingly, central RIP cell ablation in our $RIP_{HER}^{DTR}$ mice led to rapid hypophagia, resulting in loss of body weight that was due to a reduction in fat mass and not in lean mass, thus clarifying the orexigenic role of central $RIP_{HER}$ cells. Moreover, we show that although body weight is decreased, fasting glucose concentrations as well as performance in a glucose tolerance test is unchanged, suggesting that central $RIP_{HER}$ cells are not necessary for maintenance of glucose homeostasis.

To date, previous studies have not been able to clearly define hypothalamic RIP cells as either orexigenic or anorexigenic. Interestingly, application of the α-MSH analog MTII was reported to increase firing of identified $RIP_{MAG}$ cells, as did insulin treatment, indicating that $RIP_{MAG}$ neurons might mediate some of the effect of α-MSH and insulin, which is to reduce food intake and body weight (22). Moreover, mice with hypothalamic $RIP_{MAG}$ cell-specific STAT3 deletion are overweight, even after transplantation of wild-type β-cells (23). However, mice lacking fatty acid synthase specifically in $RIP_{MAG}$ cells are lean, suggesting that disturbance of $RIP_{MAG}$ cell function would lead to hypophagia (29). In our model, expression of the major hypothalamic neuropeptides in control of body weight (such as POMC, AgRP, or NPY) is unlikely to mediate the effect of $RIP_{HER}$ cell ablation because none of these neuropeptides is drastically altered following ablation. The change in ratio between orexigenic and anorexigenic neuropeptide expression might at least partially be due to decreased serum leptin concentrations secondary to decreased fat mass; however, it could also be interpreted as the physiologic counter regulatory response to the overall anorexic drive. However, the fact that acute ablation of $RIP_{HER}$ neurons results in increased activation of PVN neurons suggests that the mechanism by which $RIP_{HER}$ neurons exert their orexigenic function is inhibition of anorexigenic PVN neurons (Fig. 4*C*). This hypothesis is further substantiated by our finding that traces of synaptic transmission of $RIP_{HER}$ neurons are detected in second-order neurons of the PVN. The fact that in addition to the PVN, the DMH also receives synaptic input from $RIP_{HER}$ cells, as shown by specific WGA immunoreactivity in $RIP_{HER}^{WGA}$ mice, is another intriguing finding that certainly deserves further analysis. In summary, our results clearly argue for the importance of $RIP_{HER}$ neurons in modulating the anorexigenic action of PVN neurons independent of AgRP- and POMC-expressing cells, and provide further opportunity for study.

Currently, there are several RIP-Cre models that allow islet development and function to be studied (25, 30, 31). However, all these models show differential patterns of neuronal expression (24). For example, one RIP-Cre mouse line from the Magnuson laboratory (31) appears to have more widespread expression of Cre in the hypothalamus and other brain regions, based upon crosses to reporter mice (29). Moreover, one study reported altered glucose tolerance in this line, even in the absence of any loxP-flanked allele crossed in Lee et al. (32). For our studies, we chose the $RIP_{HER}$-Cre line first described by Herrera (25). This line has been reported to show scattered Cre expression, especially in the nuclei of the mediobasal hypothalamus (25). Staining for GFP in $RIP_{HER}^{GFP}$ mice confirmed this pattern, with most of the Cre-positive neurons located in the mediobasal hypothalamus. In addition, we verified unchanged glucose tolerance and body weight between wild-type mice and mice carrying only the $RIP_{HER}$-Cre transgene. Though the exact nature of hypothalamic RIP-Cre neurons identified by the different lines clearly remains to be determined, our data reveal that the $RIP_{HER}$-Cre neurons unexpectedly represent a functionally relevant distinct population of orexigenic hypothalamic neurons. Further experiments must thus aim to identify the molecular mechanisms underlying the role of RIP cells in the hypothalamus, i.e., through further detailed analysis of their gene expression signatures and the identification of the physiological regulators of their activity, such as nutrient sensing hormones or direct nutrient signaling as such elucidated by glucose or fatty acids. Deeper fundamental knowledge in this area will be instrumental for deciphering the neurobiological regulation of energy homeostasis and for identifying drug targets for the treatment of obesity.

## Materials and Methods

**Animal Care.** Care of all animals was within institutional animal care committee guidelines, and all animal experiments were approved by the local government (Landesamt für Natur, Umwelt und Verbraucherschutz North Rhine Westphalia), and carried out according to the National Institutes of Health's *Guide for the Care and Use of Laboratory Animals* (33). Mice were housed in groups of 3–5 at 22–24 °C using a 12:12-h light/dark cycle with lights on at 6:00 AM. Animals were fed regular chow food (Teklad Global Rodent no. T.2018.R12) containing 53.5% of carbohydrates, 18.5% of protein, and 5.5% of fat (12% of calories from fat; Harlan Teklad), and had ad libitum access to water at all times.

**Generation of $POMC^{DTR}$, $POMC^{LacZ}$, $POMC^{DTR/LacZ}$, $RIP_{HER}^{DTR}$, $RIP_{HER}^{GFP}$, $RIP_{HER}^{DTR/GFP}$, and $RIP_{HER}^{WGA}$ Mice.** POMC-Cre mice (34) were mated with $DTR^{+/-}$ mice (13), and a breeding colony was maintained by mating resulting double-heterozygous ($POMC^{DTR}$) mice with wild-type mice. POMC-Cre and $POMC^{DTR}$ mice were mated with *RosaArte1* reporter mice (LacZ) and resulted in double-heterozygous ($POMC^{LacZ}$) and triple -heterozygous ($POMC^{DTR/LacZ}$) mice. We used the same strategy to generate the various $RIP_{HER}$ mice using mice that express Cre under the control of the RIP (25), except using Z/EG (GFP) (26) reporter mice instead of lacZ reporter mice. In addition, $RIP_{HER}$-Cre mice were crossed with iZ/WAP mice (27). Only animals from the same mixed background strain generation were compared with each other. Animals were genotyped for the presence of various transgenes by PCR on DNA isolated from tail biopsies as previously described (13, 18). Mice exhibiting detectable deletion of the DTR-STOP cassette indicative of germ line or mosaic deletion were immediately killed and not included in the study.

**Icv Cannula Placement and DT Treatment.** Icv cannulation was performed as described recently (35, 36). Briefly, a sterile osmotic pump connector cannula (Bilaney Consultants GmbH) was implanted into the lateral brain ventricle (0.2 mm anterior and 1.0 mm lateral relative to Bregma and 2.3 mm below the surface of the skull) of anesthetized mice using a stereotactic device. The support plate of the catheter was attached to the skull with superglue. The catheter was prefilled with 0.9% NaCl and connected to a Micro-Renathane catheter (MRE-025; Braintree Scientific, Inc.). After 7 d of recovery, 4 μL of DT (Sigma-Aldrich; D0564; 0.15 μg/mL solved in 0.9% NaCl) was injected into the icv catheter. A total of 1 μL of 0.9% NaCl was postinjected to ensure complete drug administration to the brain. Icv injections were performed under isoflurane anesthesia 1 h after onset of the light cycle. Animals that received icv DT treatment simultaneously received ip injection of 0.9% NaCl (10 μL/g body weight) to ensure equal handling conditions with ip DT-treated animals. For ip treatment, the mice received 40 ng/g body weight of DT (4 μg/mL in 0.9% NaCl) ip after 7 d of recovery. To ensure equal handling conditions, 4 μL of 0.9% NaCl were simultaneously injected into the icv catheter.

**Analytical Procedures.** Blood glucose values were determined from whole venous blood using an automatic glucose monitor (GlucoMen; Menarini Diagnostics). Serum leptin and corticosterone were measured by ELISA using mouse standards according to the manufacturer's guidelines (Mouse Leptin ELISA, 90030; Crystal Chem; Corticosterone EIA Kit no. 900-097; Assay Designs).

**mRNA Quantification.** Measurements of mRNA levels were carried out by quantitative RT-PCR on RNA extracted from dissected hypothalamic and pituitary tissue. Total RNA for each hypothalamus/pituitary was quantified by spectrophotometry after purification using TRIzol reagent (PEQLAB Biotechnologie). A total of 200 ng of each total RNA sample was reverse-transcribed and PCR-amplified using TaqMan Principles ABI Prism 7700 Sequence Detection System (Applied Biosystems). Efficiency for the primers was estimated from standard curves made with serial cDNA dilutions.

**Tissue Preparation and Immunohistochemical Procedures.** $POMC^{DTR/LacZ}$, $RIP_{HER}^{DTR/GFP}$, $RIP_{HER}^{WGA}$ reporter, and the respective wild-type control mice were anesthetized and then perfused transcardially with 40 mL of 4% (4g/100mL) paraformaldehyde (PFA) in 0.1 M PBS (pH 7.4). The hypothalami and pituitaries were dissected and soaked in 20% sucrose overnight for cryoprotection, after which 25-μm-thick free-floating coronal sections were cut through the PVN and the ARC using a freezing microtome (Leica Microsystems). The sections were treated with 1.0% sodium borohydride for 30 min, then 0.5% Triton X-100 in 0.5% $H_2O_2$ in PBS for 15 min, and finally in

2% normal horse serum in PBS to block the nonspecific antibody binding. Following pretreatments, lacZ sections were placed in sheep α–β-gal antiserum at 1:16,000 dilution for 2 d at 4 °C, followed by treatment in Cy3-conjugated donkey anti-sheep IgG (1:100; Jackson ImmunoResearch Laboratories) for 2 h. After rinsing in PBS, the sections were mounted and coverslipped with Vectashield mounting medium (Vector Laboratories). For GFP, c-Fos, and WGA stainings, mice were perfused with saline solution followed by 4% paraformaldehyde in 0.1 M PBS (pH 7.4). Hypothalami were dissected, postfixed in 4% paraformaldehyde at 4 °C, transferred to 20% sucrose for 6 h, and frozen in tissue-freezing medium. The 25-μm-thick sections were collected in PBS/azide (pH 7.4), washed extensively to remove cryoprotectant, and then stained using previously described standard protocols (27, 37, 38). Brain sections were incubated overnight at 4 °C in primary antibodies [rabbit anti-GFP, 1:10,000 (Invitrogen/Molecular Probes); rabbit α–c-Fos, 1:20,000 (EMD Bioscience, Merck KGaA); goat anti-WGA, 1:500 (Vector)] and then visualized by different species-specific detection antibodies. For GFP and c-Fos, sections were extensively washed in PBS, incubated for 2 h at room temperature in biotinylated anti-rabbit antibody (Vector; 1:200), washed again, and then incubated in ABC solution for 1 h at room temperature (37). Sections were then rinsed in PBS, incubated in 3,3′-Diaminobenzidine (DAB) (0.4%) and $H_2O_2$ (0.01%) for 4–6 min, rinsed again, mounted onto gelatin-coated slides, dried, and finally coverslipped using mounting medium. For WGA, donkey anti-goat tetramethylrhodamine B isothiocyanate (TRITC) was used as a detection antibody (Jackson ImmunoResearch; 1:250 dilution) for 60 min. Sections were examined under a Zeiss Axioplan 2 microscope outfitted with an AxioCam HRc camera and AxioVision 4.2 imaging software. Every section containing the region of interest was examined for each animal (with the operator blinded to the experimental conditions). For each hemisphere of the respective region, at a magnification of 40×, a single plane of focus was chosen. All of the c-Fos– or WGA-labeled cell nuclei were counted within the box for each section. Only those labeled nuclei that were clearly in the plane of focus were selected. The results were expressed as the number of c-Fos– or WGA-positive cells per area of the respective nuclear region.

**Statistical Analysis.** Data sets were analyzed for statistical significance using a two-tailed unpaired Student's *t* test. Over time, ANOVA was used to test significance of body weight changes and blood glucose levels during glucose tolerance testing. Displayed values are means ± SEM. $*P \leq 0.05$; $**P \leq 0.01$; $***P \leq 0.001$; and $****P \leq 0.0001$ between the indicated groups.

**ACKNOWLEDGMENTS.** We thank Bradford Lowell and Joel Elmquist for kindly providing the POMC-Cre mice. This work was supported by Deutsche Forschungsgemeinschaft (DFG) Grant BR 1492/7-1, the DFG within the Excellence Initiative of the German federal and state governments, Center for Molecular Medicine University of Cologne Grant TV A1, and the Max Planck Society (J.C.B.).

1. Belgardt BF, Brüning JC (2010) CNS leptin and insulin action in the control of energy homeostasis. *Ann N Y Acad Sci* 1212:97–113.
2. Sánchez-Lasheras C, Könner AC, Brüning JC (2010) Integrative neurobiology of energy homeostasis-neurocircuits, signals and mediators. *Front Neuroendocrinol* 31:4–15.
3. Könner AC, Klöckener T, Brüning JC (2009) Control of energy homeostasis by insulin and leptin: Targeting the arcuate nucleus and beyond. *Physiol Behav* 97:632–638.
4. Hetherington (1940) Hypothalamic lesions and adiposity in the rat. *Nutr Rev* 41(4): 124–127.
5. Teitelbaum P, Stellar E (1954) Recovery from the failure to eat produced by hypothalamic lesions. *Science* 120:894–895.
6. Kitamura D, Roes J, Kühn R, Rajewsky K (1991) A B cell-deficient mouse by targeted disruption of the membrane exon of the immunoglobulin mu chain gene. *Nature* 350: 423–426.
7. Breitman ML, et al. (1987) Genetic ablation: Targeted expression of a toxin gene causes microphthalmia in transgenic mice. *Science* 238:1563–1565.
8. Palmiter RD, et al. (1987) Cell lineage ablation in transgenic mice by cell-specific expression of a toxin gene. *Cell* 50:435–443.
9. Saito M, et al. (2001) Diphtheria toxin receptor-mediated conditional and targeted cell ablation in transgenic mice. *Nat Biotechnol* 19:746–750.
10. Buch T, et al. (2005) A Cre-inducible diphtheria toxin receptor mediates cell lineage ablation after toxin administration. *Nat Methods* 2:419–426.
11. Luquet S, Perez FA, Hnasko TS, Palmiter RD (2005) NPY/AgRP neurons are essential for feeding in adult mice but can be ablated in neonates. *Science* 310:683–685.
12. Jung S, et al. (2002) In vivo depletion of CD11c+ dendritic cells abrogates priming of CD8+ T cells by exogenous cell-associated antigens. *Immunity* 17:211–220.
13. Gropp E, et al. (2005) Agouti-related peptide-expressing neurons are mandatory for feeding. *Nat Neurosci* 8:1289–1291.
14. Boston BA, Cone RD (1996) Characterization of melanocortin receptor subtype expression in murine adipose tissues and in the 3T3-L1 cell line. *Endocrinology* 137:2043–2050.
15. An JJ, et al. (2007) Peripheral effect of alpha-melanocyte-stimulating hormone on fatty acid oxidation in skeletal muscle. *J Biol Chem* 282:2862–2870.
16. Coll AP, Farooqi IS, Challis BG, Yeo GS, O'Rahilly S (2004) Proopiomelanocortin and energy balance: Insights from human and murine genetics. *J Clin Endocrinol Metab* 89:2557–2562.
17. Smart JL, Tolle V, Low MJ (2006) Glucocorticoids exacerbate obesity and insulin resistance in neuron-specific proopiomelanocortin-deficient mice. *J Clin Invest* 116:495–505.
18. Belgardt BF, et al. (2008) PDK1 deficiency in POMC-expressing cells reveals FOXO1-dependent and -independent pathways in control of energy homeostasis and stress response. *Cell Metab* 7:291–301.
19. Jacobson L (1999) Glucocorticoid replacement, but not corticotropin-releasing hormone deficiency, prevents adrenalectomy-induced anorexia in mice. *Endocrinology* 140:310–317.
20. Dallman MF, et al. (2003) A spoonful of sugar: Feedback signals of energy stores and corticosterone regulate responses to chronic stress. *Physiol Behav* 79:3–12.
21. Gannon M, Shiota C, Postic C, Wright CV, Magnuson M (2000) Analysis of the Cre-mediated recombination driven by rat insulin promoter in embryonic and adult mouse pancreas. *Genesis* 26:139–142.
22. Choudhury AI, et al. (2005) The role of insulin receptor substrate 2 in hypothalamic and beta cell function. *J Clin Invest* 115:940–950.
23. Cui Y, et al. (2004) Essential role of STAT3 in body weight and glucose homeostasis. *Mol Cell Biol* 24:258–269.
24. Schwartz MW, Guyenet SJ, Cirulli V (2010) The hypothalamus and β-cell connection in the gene-targeting era. *Diabetes* 59:2991–2993.
25. Herrera PL (2000) Adult insulin- and glucagon-producing cells differentiate from two independent cell lineages. *Development* 127:2317–2322.
26. Novak A, Guo C, Yang W, Nagy A, Lobe CG (2000) Z/EG, a double reporter mouse line that expresses enhanced green fluorescent protein upon Cre-mediated excision. *Genesis* 28:147–155.
27. Louis GW, Leinninger GM, Rhodes CJ, Myers MG, Jr. (2010) Direct innervation and modulation of orexin neurons by lateral hypothalamic LepRb neurons. *J Neurosci* 30: 11278–11287.
28. Braz JM, Rico B, Basbaum AI (2002) Transneuronal tracing of diverse CNS circuits by Cre-mediated induction of wheat germ agglutinin in transgenic mice. *Proc Natl Acad Sci USA* 99:15148–15153.
29. Chakravarthy MV, et al. (2007) Brain fatty acid synthase activates PPARalpha to maintain energy homeostasis. *J Clin Invest* 117:2539–2552.
30. Dor Y, Brown J, Martinez OI, Melton DA (2004) Adult pancreatic beta-cells are formed by self-duplication rather than stem-cell differentiation. *Nature* 429:41–46.
31. Postic C, et al. (1999) Dual roles for glucokinase in glucose homeostasis as determined by liver and pancreatic beta cell-specific gene knock-outs using Cre recombinase. *J Biol Chem* 274:305–315.
32. Lee JY, et al. (2006) RIP-Cre revisited, evidence for impairments of pancreatic beta-cell function. *J Biol Chem* 281:2649–2653.
33. Committee on Care and Use of Laboratory Animals (1985) *Guide for the Care and Use of Laboratory Animals* (Natl Inst Health, Bethesda), DHHS Publ No (NIH) 85–23.
34. Balthasar N, et al. (2004) Leptin receptor signaling in POMC neurons is required for normal body weight homeostasis. *Neuron* 42:983–991.
35. Belgardt BF, et al. (2010) Hypothalamic and pituitary c-Jun N-terminal kinase 1 signaling coordinately regulates glucose metabolism. *Proc Natl Acad Sci USA* 107: 6028–6033.
36. Kleinridders A, et al. (2009) MyD88 signaling in the CNS is required for development of fatty acid-induced leptin resistance and diet-induced obesity. *Cell Metab* 10:249–259.
37. Plum L, et al. (2007) Enhanced leptin-stimulated Pi3k activation in the CNS promotes white adipose tissue transdifferentiation. *Cell Metab* 6:431–445.
38. Janoschek R, et al. (2006) gp130 signaling in proopiomelanocortin neurons mediates the acute anorectic response to centrally applied ciliary neurotrophic factor. *Proc Natl Acad Sci USA* 103:10707–10712.